magnetochemistry

MDPI

Article

Cell Behavioral Changes after the Application of Magneto-Mechanical Activation to Normal and Cancer Cells

Aikaterini-Rafailia Tsiapla [1,2,*,†], Veselina Uzunova [3,†], Tsvetelina Oreshkova [4], Makis Angelakeris [1,2], Theodoros Samaras [1,2], Orestis Kalogirou [1,2] and Rumiana Tzoneva [3,*]

1 Faculty of Sciences, School of Physics, Aristotle University, 54124 Thessaloniki, Greece; agelaker@auth.gr (M.A.); theosama@physics.auth.gr (T.S.); kalogiro@physics.auth.gr (O.K.)
2 Center for Interdisciplinary Research and Innovation (CIRI-AUTH), Magna Charta, 57001 Thessaloniki, Greece
3 Laboratory of Transmembrane Signaling, Institute of Biophysics and Biomedical Engineering, Bulgarian Academy of Sciences, Acad. G. Bonchev Street, Block 21, 1113 Sofia, Bulgaria; vesi.uzunova@abv.bg
4 Institute of Biology and Immunology of Reproduction "Academician Kiril Bratanov", Bulgarian Academy of Sciences, 73 Tsarigradsko Shose, 1113 Sofia, Bulgaria; tsveti_oreshkova@yahoo.com
* Correspondence: aitsiapl@physics.auth.gr (A.-R.T.); tzoneva@bio21.bas.bg (R.T.)
† These authors contributed equally to this work.

Abstract: In vitro cell exposure to nanoparticles, depending on the applied concentration, can help in the development of theranostic tools to better detect and treat human diseases. Recent studies have attempted to understand and exploit the impact of magnetic field-actuated internalized magnetic nanoparticles (MNPs) on the behavior of cancer cells. In this work, the viability rate of MNP's-manipulated cancerous (MCF-7, MDA-MB-231) and non-cancerous (MCF-10A) cells was investigated in three different types of low-frequency magnetic fields: static, pulsed, and rotating field mode. In the non-cancerous cell line, the cell viability decreased mostly in cells with internalized MNPs and those treated with the pulsed field mode. In both cancer cell lines, the pulsed field mode was again the optimum magnetic field, which together with internalized MNPs caused a large decrease in cells' viability (50–55% and 70% in MCF-7 and MDA-MB-231, respectively) while the static and rotating field modes maintained the viability at high levels. Finally, F-actin staining was used to observe the changes in the cytoskeleton and DAPI staining was performed to reveal the apoptotic alterations in cells' nuclei before and after magneto-mechanical activation. Subsequently, reduced cell viability led to a loss of actin stress fibers and apoptotic nuclear changes in cancer cells subjected to MNPs triggered by a pulsed magnetic field.

Keywords: magneto-mechanical activation; magnetic nanoparticles; breast cancer cell lines; cytotoxicity; cytoskeleton; DAPI staining

Citation: Tsiapla, A.-R.; Uzunova, V.; Oreshkova, T.; Angelakeris, M.; Samaras, T.; Kalogirou, O.; Tzoneva, R. Cell Behavioral Changes after the Application of Magneto-Mechanical Activation to Normal and Cancer Cells. *Magnetochemistry* **2022**, *8*, 21. https://doi.org/10.3390/magnetochemistry8020021

Academic Editor: Salah Massoud

Received: 29 December 2021
Accepted: 29 January 2022
Published: 1 February 2022

1. Introduction

Breast cancer is the leading cause of death, competing against cardiovascular disease, and the most diagnosed cancer among women worldwide [1]. Many studies have focused on the development of new anticancer drugs, paving the pathway for subsequent in vivo and clinical trials [2]. To reduce undesirable secondary effects, several studies [3,4] have been reported the use of radio-frequency (RF) magnetic field and magnetic nanoparticles (MNPs) in magnetic hyperthermia to destroy cancer cells, as MNPs allow the selective delivery of a therapeutic agent to the target. However, a lot of issues need to be addressed, such as the biological mechanisms of cells that take place after a temperature increase above 41 °C, which are not fully understood [3,4].

The magneto-mechanical effect of nanoparticles is a relatively new field of research for cancer treatment [5], in which mechanical forces that are generated via magnetic fields manipulate MNPs inside variable environments [6–8]. Magnetic energy is converted

into mechanical energy, combining different magnetic field configurations (such as static, pulsed, rotating) of very low frequencies with MNPs, allowing them to function and bind specifically to cell membranes (malignant and non-malignant) and destroy only the cancer tissues [9,10]. A recent review reports that disc-shaped magnetic particles have been proven to be excellent magneto-mechanical actuators, leading cancer cells to apoptosis through self-destruction [11]. More specifically, Goiriena-Goikoetxea et al. compared the torque and dispersion capability of different types of magnetic discs to find the most efficient magneto-mechanical actuator [11].

Zhang et al. [12] designed and exposed cells under a rotating magnetic field generator of very low frequency (10–40 Hz). They used iron oxide nanoparticles coated, for instance, with antibodies against LAMP-1 (lysosomal-associated membrane protein), which enhanced internalization and loading into the lysosomes. After the treatment, the authors reported a rapid decrease in the size and number of lysosomes. Therefore, they observed lysosomal membrane disruption (lysosomal integrity destruction and lysosomal enzyme leakage), which in turn induced cell death.

Kim et al. created a magneto-mechanical device and exposed cells under an alternating magnetic field (AMF) of low frequency, 10 Hz [13]. They used disc-shaped magnetic particles biofunctionalized with anti-human-IL13α2R antibody to target human glioblastoma cells. After treatment, they observed cell morphology changes with a rounded shape, membrane shrinkage, and loss of membrane integrity. Therefore, they supposed that programmed cell death pathways were activated.

Spyridopoulou et al. used a 3D tunable magneto-mechanical device, which was designed and manufactured by Maniotis et al. [9], to generate either a static or alternating magnetic field with varying intensity (40–200 mT) and frequency (0–8 Hz) and showed that cytoskeletal disruption was altered in HT29 cancer cells after magnetic field actuation [10].

In the present study, we focused on the exposure of MNPs-treated or untreated MCF-10A non-cancerous cells and MCF-7 and MDA-MB-231 cancer cells with various magnetic field modes with the same 3D tunable magneto-mechanical device described in [9]. Specifically, to apply mechanical stress in cells, we used MNPs with a hydrodynamic diameter of 100 nm, guided either by static, pulsed, or rotating field modes at an extremely low frequency of 2 Hz and amplitude of 200 mT. For the static and pulsed field modes, two cell culture dishes containing the aforementioned cells with and without MNPs were placed on top of a static holder (one on the left and one on the right side of the holder) above the turntable. For the pulsed field mode, permanent magnets (commercial Nd-Fe-B block magnets) rotated around the dishes, in contrast with the static field mode, where the magnets were static. For the rotating field mode, one dish each time was placed at the center of the holder above turntable and the permanent magnets rotated around it. Finally, it is worth noting that in extremely low-frequency (ELF) electromagnetic fields, such as the magneto-mechanical treatment, which is suggested in our study, no temperature increase is induced in the sample under study, as in contrast to magnetic hyperthermia, magneto-mechanical activation is a non-heating magnetic field technique [14,15].

2. Materials and Methods

2.1. Materials

The magnetic nanoparticles used in this work were supplied by Chemicell GmbH, Germany (fluid MAG-D, Art №4101). Fluid MAG-D nanoparticles consist of aqueous dispersions of magnetic iron oxides with an average hydrodynamic diameter of 100 nm and a multi-domain core. Their iron oxide core is covered with a hydrophilic polymer matrix (starch) to protect them against aggregation by foreign ions [16].

Chemicals were purchased from Sigma-Aldrich (St. Louis, MO, USA): Phalloidin-TRITC (P1951), 4,6-diamidino-2-phenylindole (DAPI, D9542).

2.2. Cell Lines

Breast tumor cell lines MCF-7 (ATCC® HTB-22™, Manassas, VA, USA) and MDA-MB-231 (ATCC® HTB-26™, Manassas, VA, USA) and the non-tumorigenic cell line MCF-10A (ATCC, CRL-10317, Manassas, VA, USA) were cultivated in 25 cm^2 cell culture flasks (Greiner Bio-One CELLSTAR). MDA-MB-231 cancer cells were cultivated in DMEM (AT186, HiMedia™ Laboratories, GmbH, Einhausen, Hessen, Germany) containing 10% FBS, L-Glutamine, and Penicillin-Streptomycin-Amphotericin B. MCF-7 cells were cultivated in DMEM containing the same supplements plus sodium pyrovate, non-essential amino acids (NEAA), and insulin. The MCF-10A cell line was cultivated in DMEM-F12 medium (AT189, HiMedia™ Laboratories, GmbH, Einhausen, Hessen, Germany) supplemented with insulin, hydrocortisone (stock solution 50 μg mL^{-1}, Merck, Darmstadt, Germany), and human epidermal growth factor (hEGF stock solution 10 ng mL^{-1}, Merck, Germany). All cell lines were cultured in a CO_2 incubator under a humidified atmosphere (37 °C, 5% CO_2).

2.3. Prussian Blue Staining

To clarify the cell internalization of the MNPs, Prussian blue staining was performed as described by Makridis et al. [17]. Briefly, MNPs-treated and control cells were fixed with 3% paraformaldehyde for 15 min, then washed 3 times with PBS (1×), and incubated with a 1:1 mixture of 10% potassium ferrocyanide in distilled water and 20% hydrochloric acid for 20 min at room temperature. Cells were washed and stained with Nuclear Fast Red solution for 15 min. After washing with distilled water, optical images were taken by a microscope Olympus (BX51, Tokyo, Japan) equipped with a camera Olympus U-TV 0.63XC.

2.4. Magneto-Mechanical Treatment of Cells

Cells were seeded in petri dishes (d = 35 mm) at a density of 3 × 10^5 cells/dish. Then, cells were incubated for 24 h in a cell medium containing 100 μg/mL MNPs prior to treatment for good cell adhesion and to facilitate the ability of cells to absorb part of the nanoparticles. After that, the petri dishes were placed inside the magneto-mechanical device and were treated with 3 different field modes (static, pulsed, and rotating), with a field amplitude of 200 mT and a field exposure time of 30 min.

2.5. MTT Test

The cytotoxicity of the magneto-mechanical treatment without or with the presence of MNPs (static, static with (+) MNPs, pulsed, pulsed with (+) MNPs, rotating, rotating with (+) MNPs) inside the 3 cell lines (MCF-10A, MCF-7, and MDA-MB-231) was evaluated by the MTT test (3-(4,5-dimethylthiazol-2-yl)-2,5-diphenyl tetrazolium bromide, Invitrogen, Waltham, MA, USA) described by Uzunova et al. [13]. Briefly, after treatment, as it is described above, the cells were incubated for different time points (24, 48, or 120 h) to track the short-term and long-term changes in cell viability. The MTT data were normalized to the control data, which were obtained for the non-treated cells (control cells without (−) MNPs).

2.6. Double Staining for F-Actin and Cell Nuclei

Pulsed magnetic field (PMF) and rotating magnetic field (RMF)-treated cells were grown on 12 mm coverslips placed in 24-well plates in a complete cell medium. Next, cells were gently washed with phosphate-buffered saline, pH 7.3 (PBS), and their F-actin cytoskeletons were stained with Phalloidin-TRITC (1:100) dye for 30 min. After triple rinsing with PBS, their nuclei (DNA) were stained with DAPI solution (1 μg/mL final concentration) for 5 min. The coverslips with the stained cells were observed on a fluorescent microscope Carl Zeiss JENA Jenalumar (Carl Zeiss, Oberkochen, Germany), equipped with a Jenoptik camera (ProgRes, SpeedXT core 3: JENOPTIK Optical Systems GmbH, Jena, Germany) and objective HI100×/1.30 oil. The images were taken at different time points: 48 and 120 h.

3. Results and Discussion

3.1. MNPs Internalization

Prior to the magneto-mechanical activation of MCF-10A and MDA-MB-231 cells, the Prussian blue technique was used to visualize whether the MNPs were internalized within the cells. Figures 1A and 2A present the optical images of MCF-10A and MDA-MB-231 control cells (without MNPs), respectively. Figures 1B and 2B depict the optical images of MCF-10A and MDA-MB-231 after 24 h of incubation of MNPs, respectively. As it is observed, in both cell lines, MNPs were efficiently labeled with blue color, proving their internalization within the cells (especially in the inset images).

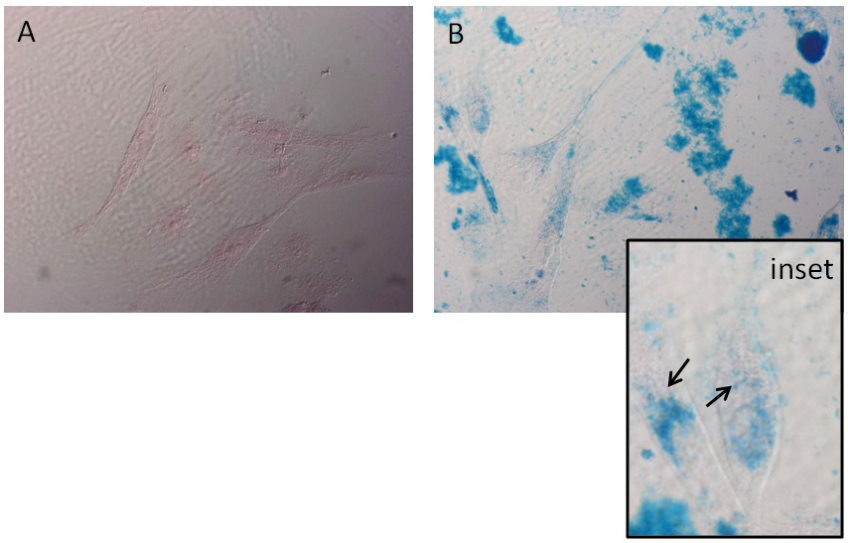

Figure 1. Prussian blue staining results of MCF-10A cells: (**A**) control cells, which correspond to the cells that were not treated with MNPs; and (**B**) cells after 24 h of incubation with MNPs, which were stained with Prussian blue reaction and visualized by optical microscopy imaging at 20× magnification. Inset: the enlarged images of internalized MNPs (arrows) on MCF-10A cells. Blue: MNPs; Red: nucleus of cells.

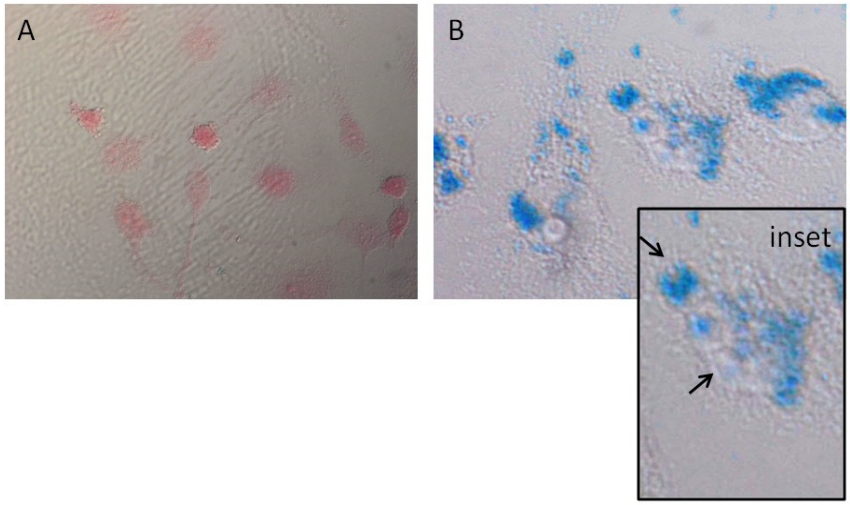

Figure 2. Prussian blue staining results of MDA-MB-231 cells: (**A**) control cells, which correspond to the cells that were not treated with MNPs; and (**B**) cells after 24 h incubation with MNPs, which were stained with Prussian blue reaction and visualized by optical microscopy imaging at 20× magnification. Inset: the enlarged images of internalized MNPs (arrows) on MDA-MB-231 cells. Blue: MNPs; Red: nucleus of cells.

3.2. Magneto-Mechanical Activation

In our earlier study [18], we showed that a 100 μg/mL concentration of magnetic nanoparticles did not cause cytotoxicity or block cell motility. Therefore, this concentration was chosen as a "safe" value for the subsequent in vitro studies. The MTT test helped us to assess the cytotoxicity of different magnetic fields, applied alone or in the presence of nanoparticles. MCF-10A, MCF-7 and MDA-MB-231 cells were exposed to a static, pulsed, and rotating magnetic field (intensity of 200 mT, frequency of 2 Hz) for a period of 30 min.

Figure 3 shows the effect of actuating magnetic fields (static, rotating, and pulsed) in the presence of MNPs on the viability rate of MCF-10A cells. Generally, a gradual decrease in the cell viability over time, (especially after 120 h) in treated cells (static, rotating, and pulsed field modes with MNPs) was noticed. The MNPs-treated cells via static, rotating, and pulsed field modes led to a greater reduction in the rate of cell proliferation. The pulsed field mode treatment showed the highest effect on the reduction of cell viability: 60% and 55% of the initial value, with and without the presence of MNPs, respectively. In contrast, for the static and rotating field modes, the cell viability during the 120 h of treatment with the presence of MNPs remained at approximately 75% (Figure 3).

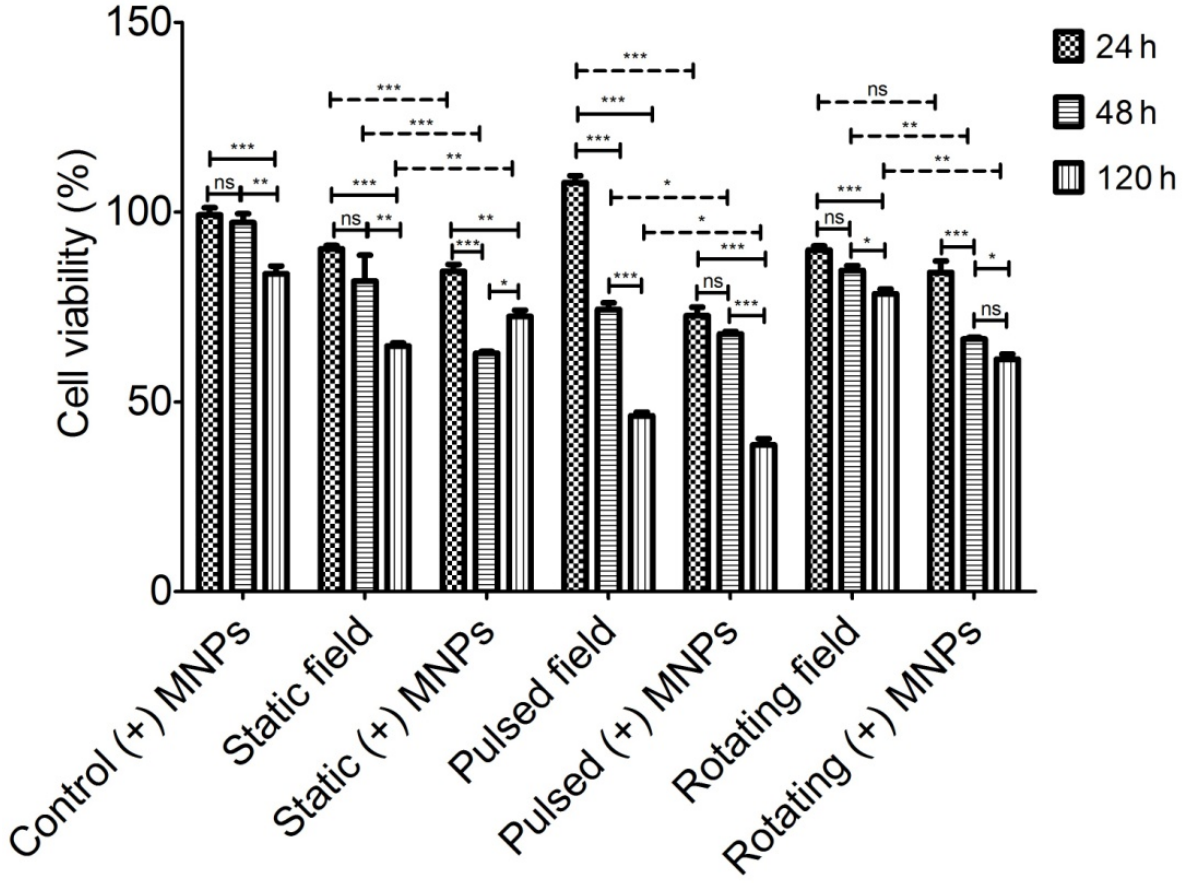

Figure 3. Effect of static, pulsed, and rotating magnetic field-actuated internalized MNPs on the growth rate of MCF-10A cells. Experiments were performed in n = 5 replicates and error bars depict the standard error of the mean. The asterisks denote a significant difference (*—$p < 0.05$, **—$p < 0.01$, ***—$p < 0.001$, ns—not significant) between different treated cells and different incubation times.

When MCF-7 cancer cells were treated with the above activation with or without the presence of internalized MNPs (Figure 4), a greater reduction in cell viability was observed again with the pulsed field mode (approximately 50–55% reduction), while for the static and rotating field modes (MNPs+ or MNPs−), the reduction in cell viability was 20–30%. Our results for MDA-MB-231 cancer cells showed an increased sensibility to the applied magneto-mechanical activation (Figure 5). For this cell line, the highest reduction in cell

viability was detected for the applied pulsed field mode with MNPs (about 70%) and unlike the other cell lines (MCF-10A, MCF-7), a significant reduction in cell viability was also detected for the rotating field mode in the presence of MNPs after 120 h of incubation (more than 50%). In all other treatments (static field mode and static field mode with MNPs and rotating field mode), the cell viability was maintained at high levels (70–100%). These observations are consistent with the work of Rinaldi et al., who have found similar results for the triple-negative breast cancer cell line MDA-MB-231 [19]. It was shown in [19] that cells under magneto-mechanical activation present significant reductions in their viability.

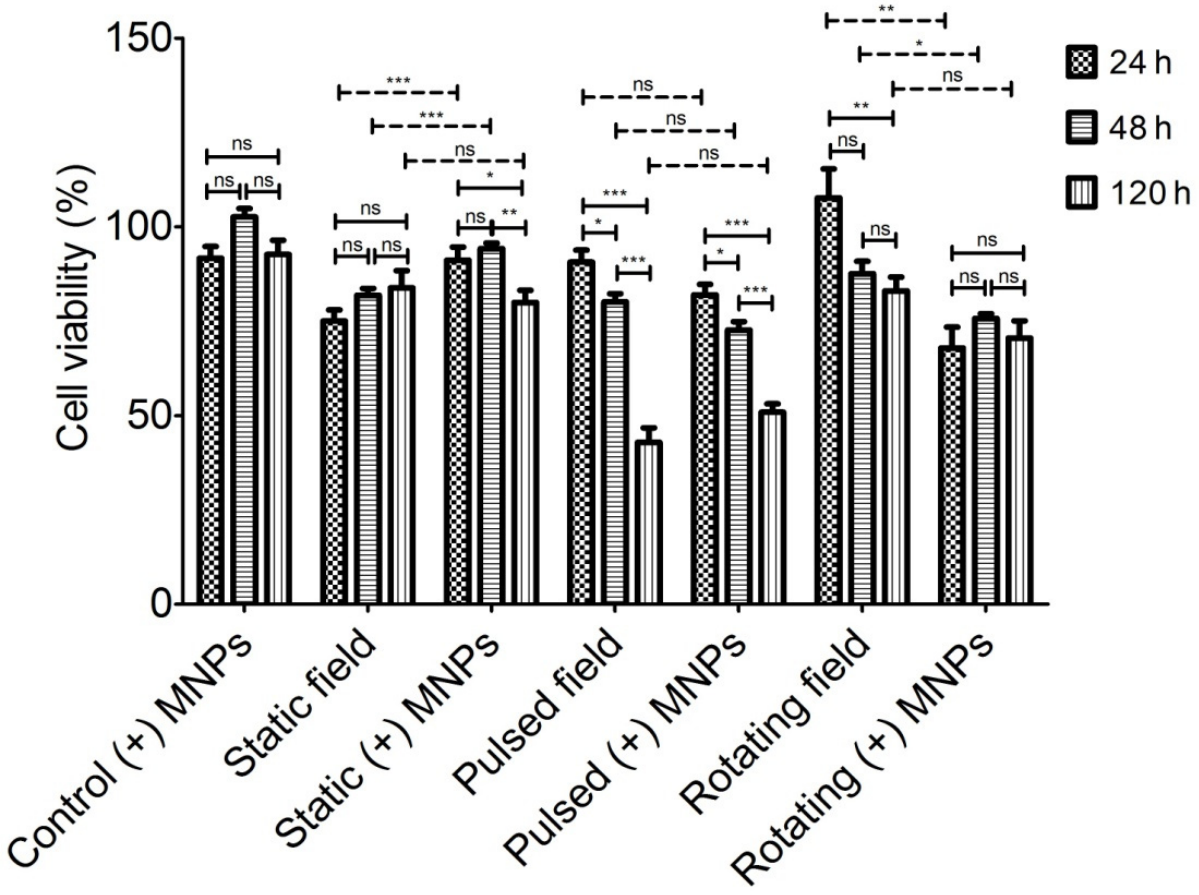

Figure 4. Effect of static, pulsed, and rotating magnetic field-actuated internalized MNPs on the growth rate of MCF-7 cells. Experiments were performed in n = 5 replicates and error bars depict the standard error of the mean. The asterisks denote a significant difference (*—$p < 0.05$, **—$p < 0.01$, ***—$p < 0.001$, ns—not significant) between different treated cells and different incubation times.

It should be noticed that the application of magnetic fields without the presence of MNPs also led to a reduction in cell viability with different intensities, especially for the non-cancerous cell line MCF-10A and non-invasive breast cancer cell line MCF-7 (Figures 3 and 4). For the MDA-MB-231 cell line, such a reduction was not observed (Figure 5). A similar effect of the extremely low-frequency electromagnetic field (ELF-EMF) on the proliferation of human breast cancer cells was observed by Wang et al. [20]. The application of MNPs facilitated the transmission of mechanical forces and thus, increased the cytotoxic effect on cell proliferation. According to the results, it can be assumed that the pulsed magnetic field in the presence of MNPs more specifically affected the cell viability of cancer cell lines (MDA-MB-231 and MCF-7) than the respective viability of the non-cancerous cell line (MCF-10A).

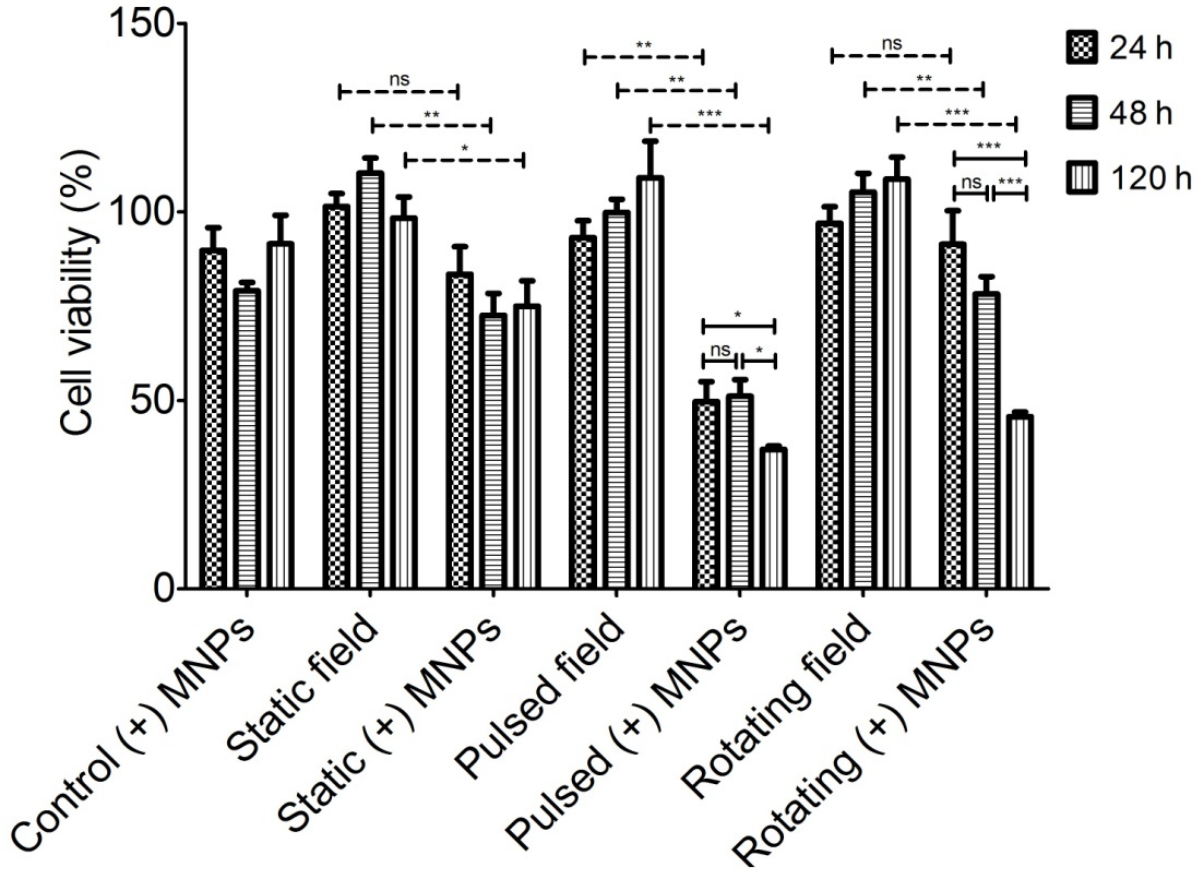

Figure 5. Effect of static, pulsed, and rotating magnetic field-actuated internalized MNPs on the growth rate of MDA-MB-231 cells. Experiments were performed in n = 5 replicates and error bars depict the standard error of the mean. The asterisks denote a significant difference (*—$p < 0.05$, **—$p < 0.01$, ***—$p < 0.001$, ns—not significant) between different treated cells and different incubation times.

3.3. Combined Effect of PMF, RMF, and MNPs on Actin Cytoskeleton and Cell Nuclei

3.3.1. Actin Cytoskeleton

The actin cytoskeleton is a sensorial network for cellular well-being and survival. It is involved in the transport and localization of cell organelles (mostly the nucleus), cell movement, cell division, etc. [21]. Different exogenously applied stimuli, such as an electromagnetic field, have been proven to affect cytoskeletal organization, the structure of subcellular compartments, and calcium flow, which may also contribute significantly to cell growth inhibition [22–30]. In the present work, the actin stress fibers of cancer and non-cancerous cell lines were visualized by TRITC-Phalloidin staining after treatment with pulsed magnetic field mode (PMF) and PMF with (48 h) incubated 100 µg/mL MNPs, as shown in Figures 6–8. From the cell viability study, a 50% decrease in the cell viability of MDA-MB-231 cells treated with rotating magnetic field mode (RMF) (+) MNPs after 120 h was observed. Therefore, the fluorescent method was followed and confirmed that after treatment with RMF (+) MNPs, marked cytoskeleton alterations were induced, Figure 9. MCF-10A cells were well spread with continuous actin networks (Figure 6A), which remained unaffected either by internalized MNPs or by the applied PMF, although MNPs partially displaced them (Figure 6B,D, white arrows). This fact proved our assumption that the selected concentration of MNPs was within reasonable "safety" limits and MNPs do not have a cytotoxic effect per se, especially in the non-cancerous cell line. For MCF-7 cancer cells, a well-organized actin cytoskeleton was noticed only in the control, as cells were growing by forming typical dome structures (Figure 7A). In contrast, all treated cells (Figure 7B–D) revealed a disturbed dome structure and altered actin organization (dot-like

structure). The MDA-MB-231 triple-negative cancer cell line also lost actin stress fibers, especially with PMF and PMF (+) MNPs, with some cumulative effects in the second one (Figure 8C,D). These data confirmed our results obtained for cell viability, since the loss of the actin cytoskeleton has a direct impact on cell viability [15]. Although the influence of the rotating field mode on the MDA-MB-231 cytoskeleton was obvious (Figure 9), this influence was found to be much weaker than that of the pulsed field mode, as it was observed that cells still possessed actin fibers (Figure 9C). The actin fibers disappeared only in the cells that were treated with the rotating field mode and (+) MNPs (Figure 9D), which also explains the diminished cell viability shown in Figure 5.

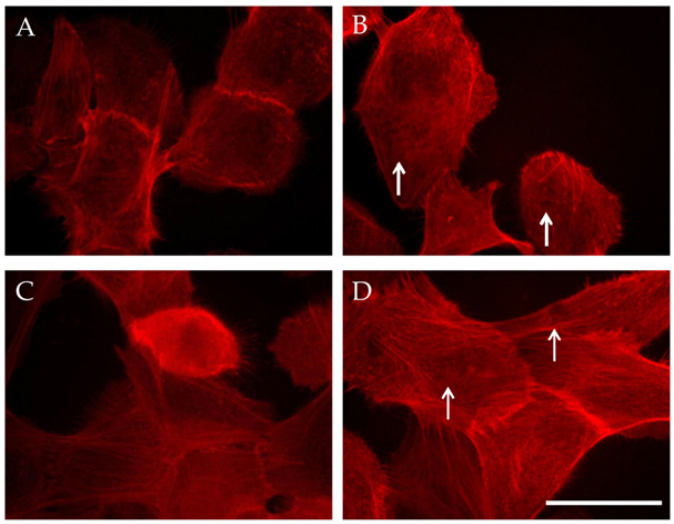

Figure 6. TRITC-Phalloidin visualization of the cell cytoskeleton in the MCF-10A cell line after 48 h of incubation. (**A**) Control cells, (**B**) cells incubated with 100 μg/mL MNPs, (**C**) PMF-treated cells, and (**D**) PMF-treated cells with the presence of 100 μg/mL MNPs. The arrows indicate the local filament reorganization and the positioning of MNPs in the cell; the bar is 50 μm.

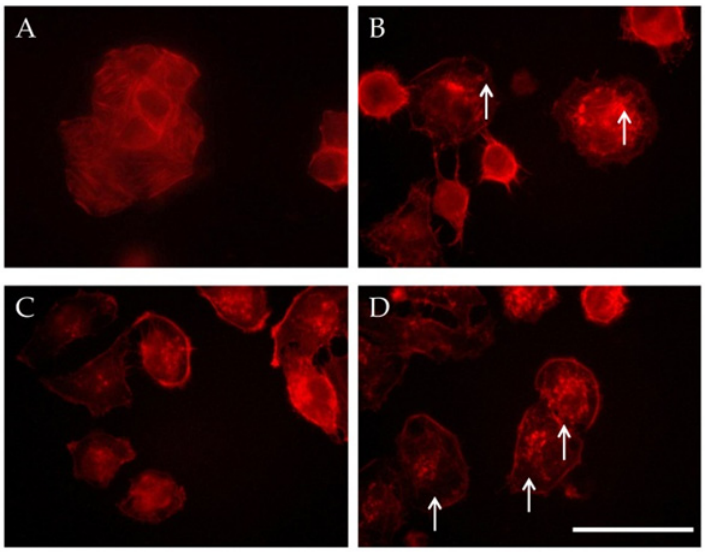

Figure 7. TRITC-Phalloidin visualization of the cell cytoskeleton in the MCF-7 cell line after 48 h of incubation. (**A**) Control cells, (**B**) cells incubated with 100 μg/mL MNPs, (**C**) PMF-treated cells, and (**D**) PMF-treated cells with the presence of 100 μg/mL MNPs. The arrows indicate the local filament reorganization and the positioning of MNPs in the cell; the bar is 50 μm.

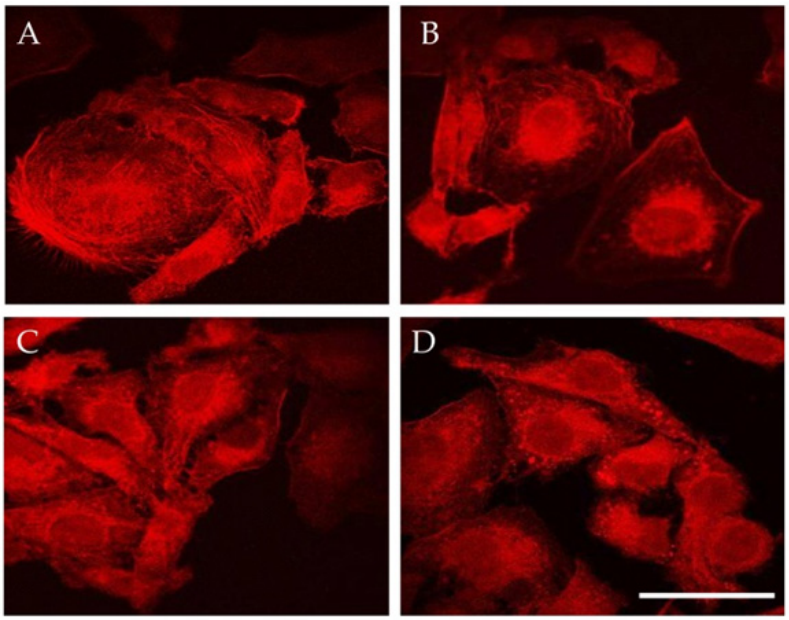

Figure 8. TRITC-Phalloidin visualization of the cell cytoskeleton in the MDA-MB-231 cell line after 48 h of incubation. (**A**) Control cells, (**B**) cells incubated with 100 μg/mL MNPs, (**C**) PMF-treated cells, and (**D**) PMF-treated cells with the presence of 100 μg/mL MNPs; the bar is 50 μm.

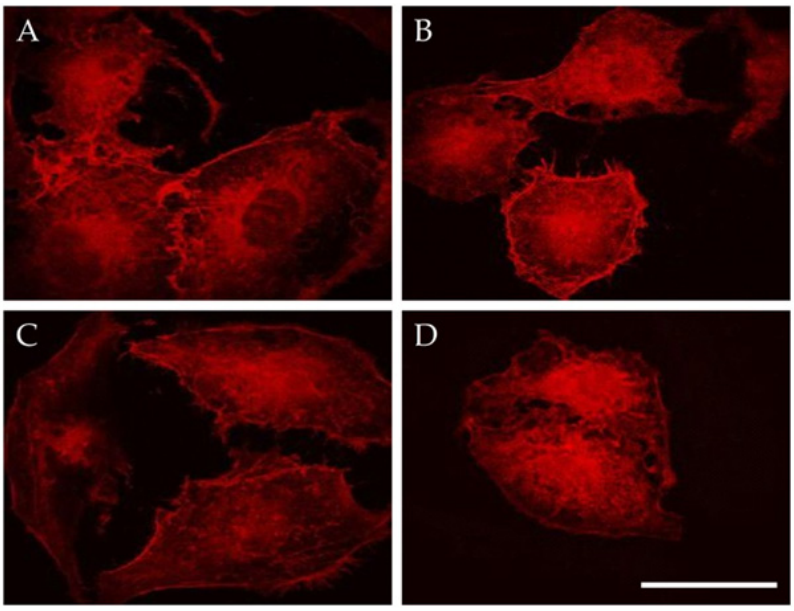

Figure 9. TRITC-Phalloidin visualization of the cell cytoskeleton in the MDA-MB-231 cell line after 120 h of incubation. (**A**) Control cells, (**B**) cells incubated with 100 μg/mL MNPs, (**C**) RMF-treated cells, and (**D**) RMF-treated cells with the presence of 100 μg/mL MNPs; the bar is 50 μm.

3.3.2. Cell Nuclei Changes

The results for MCF-10A cells showed that nanoparticles are internalized in cells, initially in the cytoplasm (data not shown), and with increasing incubation time, they accumulated in the perinuclear space (Figure 10, dark shadows in B and D). The fluorescent images indicated slightly altered nuclear morphology, expressed as the asymmetric nuclear shape of cells, which were treated with pulsed field mode without MNPs (Figure 10C) and pulsed field mode with MNPs (Figure 10D). The magneto-mechanical activation in the presence of MNPs in MCF-7 cells caused different nuclear anomalies, including an irregular form, micronuclei, and apoptotic bodies (Figure 11D), all leading to apoptosis.

MDA-MB-231 cells treated with pulsed field mode in the presence of MNPs also showed enlarged, swollen, and apoptotic nuclei (Figure 12D). In MDA-MB-231 cells that were treated with rotating field mode in the presence of MNPs, the cell nuclei exhibited an irregular form too (Figure 13D). The above results are illustrated in Figures 10–13, which present the nuclear morphology of all three cell lines, with and without the presence of MNPs, before and after magneto-mechanical treatment.

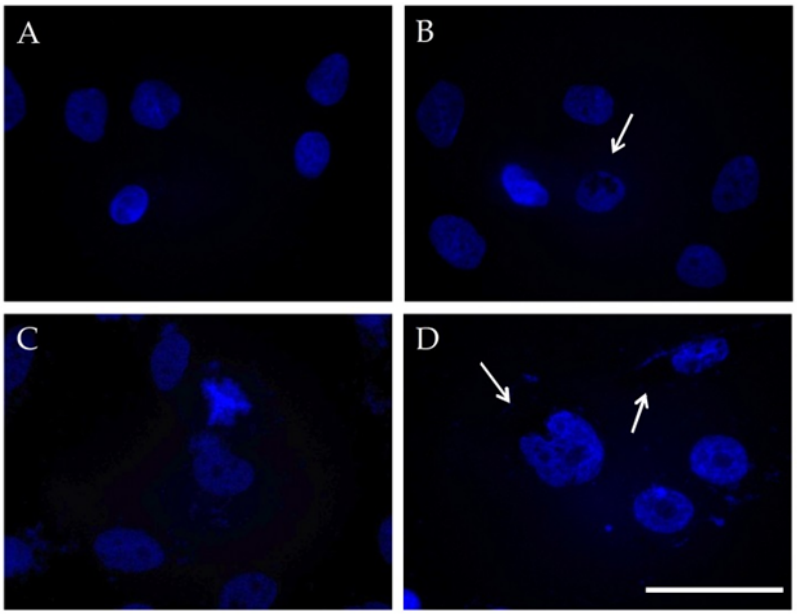

Figure 10. Nuclear morphology in the MCF-10A cell line after 48 h of incubation. (**A**) Control cells, (**B**) cells incubated with 100 μg/mL MNPs, (**C**) PMF-treated cells, and (**D**) PMF-treated cells with the presence of 100 μg/mL MNPs. The arrows indicate the morphological changes in nuclei; the bar is 50 μm.

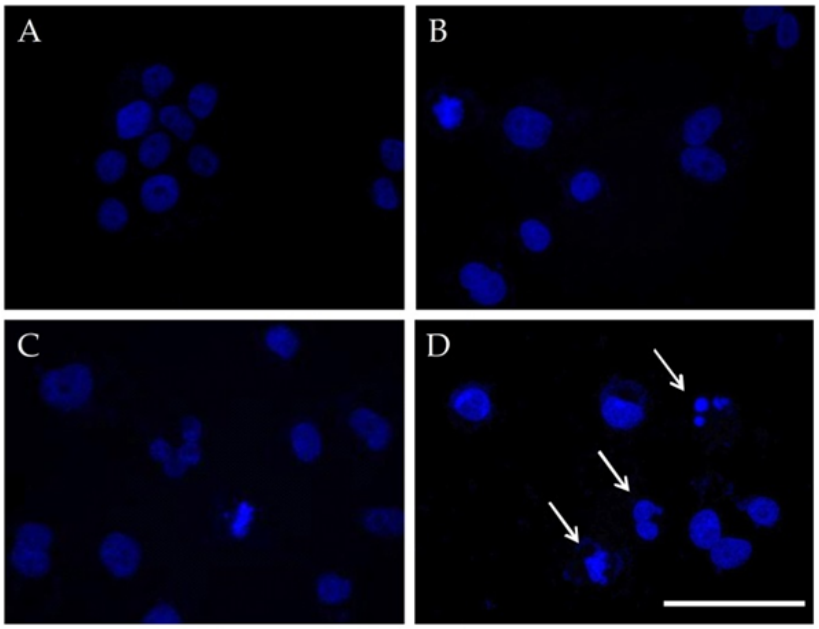

Figure 11. Nuclear morphology in the MCF-7 cell line after 48 h of incubation. (**A**) Control cells, (**B**) cells incubated with 100 μg/mL MNPs, (**C**) PMF-treated cells, and (**D**) PMF-treated cells with the presence of 100 μg/mL MNPs. The arrows indicate the morphological changes in nuclei; the bar is 50 μm.

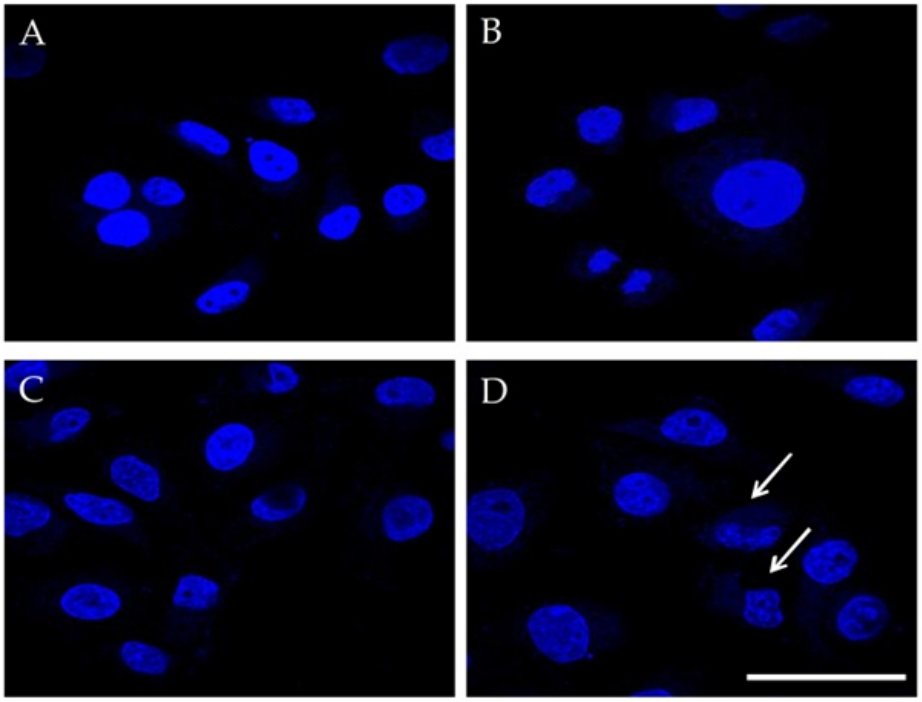

Figure 12. Nuclear morphology in the MDA-MB-231 cell line after 48 h of incubation. (**A**) Control cells, (**B**) cells incubated with 100 μg/mL MNPs, (**C**) PMF-treated cells, and (**D**) PMF-treated cells with the presence of 100 μg/mL MNPs. The arrows indicate the morphological changes in nuclei; the bar is 50 μm.

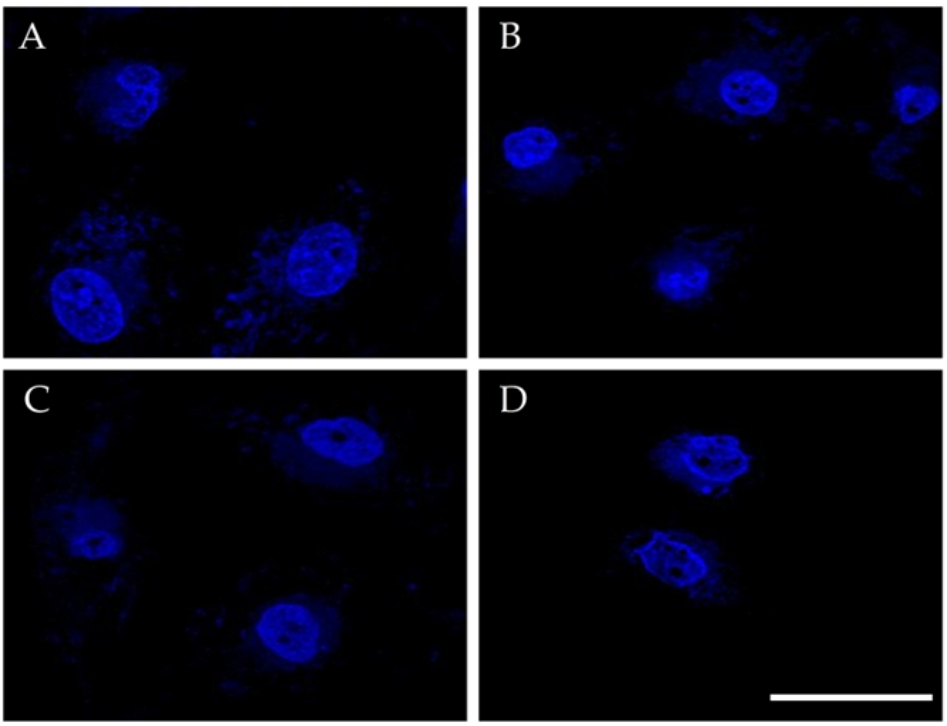

Figure 13. Nuclear morphology in the MDA-MB-231 cell line after 120 h of incubation. (**A**) Control cells, (**B**) cells incubated with 100 μg/mL MNPs, (**C**) RMF-treated cells, and (**D**) RMF-treated cells with the presence of 100 μg/mL MNPs; the bar is 50 μm.

4. Conclusions

In this work, we studied the behavioral changes in normal and breast cancer cells after the application of magnetic fields and/or magneto-mechanical activation. The cell behavior was analyzed in the presence or absence of internalized MNPs, using a novel custom-made device with a 3D-printed turntable. Cells were exposed to various magnetic field modes (static, pulsed, and rotating) in extremely low-frequency magnetic fields with an intensity of 200 mT and frequency of 2 Hz. It was observed that the pulsed magneto-mechanical forces applied through MNPs actuation decreased the viability in both MCF-7 (approximately 50–55%), and MDA-MB-231 cancer cells, especially in the triple-negative breast cancer cell line MDA-MB-231 (about 70% reduction). Therefore, the pulsed field mode was chosen as the optimum field mode for magneto-mechanical treatment, instead of the static and rotating field mode, where the cell viability was generally maintained at high levels. The diminished cell viability after the pulsed field mode was confirmed by actin stress fiber loss and apoptotic nuclear changes. However, further studies need to take place for a better understanding of the mechanisms involved.

Author Contributions: Conceptualization, M.A., T.S., O.K. and R.T.; Formal analysis, A.-R.T., V.U. and T.O.; Investigation, A.-R.T., V.U. and T.O.; Methodology, A.-R.T.; Supervision, M.A., T.S., O.K. and R.T.; Validation, A.-R.T. and V.U.; Visualization, A.-R.T. and T.O.; Writing—original draft, A.-R.T.; Writing—review & editing, R.T.; A.-R.T. and V.U. All authors have read and agreed to the published version of the manuscript.

Funding: This work was supported by the Bulgarian Ministry of Education and Science under the National Research Programme "Young scientists and postdoctoral students" approved by DCM#577/17.08.2018 and by Joint Research Project BAS-AUTH, 2018-2020.

Institutional Review Board Statement: Not applicable.

Informed Consent Statement: Not applicable.

Data Availability Statement: Not applicable

Conflicts of Interest: The authors declare no conflict of interest.

References

1. Hose, O.; Tertis, M.; Cristea, C. Implication of Magnetic Nanoparticles in Cancer Detection, Screening and Treatment. *Magnetochemistry* **2019**, *5*, 55. [CrossRef]
2. Wang, H.; Qian, J.; Zhang, Y.; Xu, W.; Xiao, J.; Suo, A. Growth of MCF-7 breast cancer cells and efficacy of anti-angiogenic agents in a hydroxyethyl chitosan/glycidyl methacrylate hydrogel. *Cancer Cell Int.* **2017**, *17*, 55. [CrossRef] [PubMed]
3. Sola-Leyva, A.; Jabalera, Y.; Chico-Lozano, M.A.; Carrasco-Jiménez, M.P.; Iglesias, G.R.; Jimenez-Lopez, C. Reactive oxygen species (ROS) production in HepG2 cancer cell line through the application of localized alternating magnetic field. *J. Mater. Chem. B* **2020**, *8*, 7667–7676. [CrossRef] [PubMed]
4. Vurro, F.; Jabalera, Y.; Mannucci, S.; Glorani, G.; Sola-Leyva, A.; Gerosa, M.; Romeo, A.; Romanelli, M.; Malatesta, M.; Calderan, L.; et al. Improving the Cellular Uptake of Biomimetic Magnetic Nanoparticles. *Nanomaterials* **2021**, *11*, 766. [CrossRef]
5. Hepel, M. Magnetic Nanoparticles for Nanomedicine. *Magnetochemistry* **2020**, *6*, 3. [CrossRef]
6. Sarella, A.; Torti, A.; Donolato, M.; Pancaldi, M.; Vavassori, P. Two-dimensional programmable manipulation of magnetic nanoparticles on-chip. *Adv. Mater.* **2014**, *26*, 2384–2390. [CrossRef]
7. Chen, L.; Chen, C.; Wang, P.; Song, T. Mechanisms of Cellular Effects Directly Induced by Magnetic Nanoparticles under Magnetic Fields. *J. Nanomater.* **2017**, *2017*, 1564634. [CrossRef]
8. Subramanian, M.; Miaskowski, A.; Jenkins, S.I.; Lim, J.; Dobson, J. Remote manipulation of magnetic nanoparticles using magnetic field gradient to promote cancer cell death. *Appl. Phys. A* **2019**, *125*, 226. [CrossRef]
9. Maniotis, N.; Makridis, A.; Myrovali, E.; Theopoulos, A.; Samaras, T.; Angelakeris, M. Magneto-mechanical action of multimodal field configurations on magnetic nanoparticle environments. *J. Magn. Magn. Mater.* **2019**, *470*, 6–11. [CrossRef]
10. Spyridopoulou, K.; Makridis, A.; Maniotis, N.; Karypidou, N.; Myrovali, E.; Samaras, T.; Angelakeris, M.; Chlichlia, A.; Kalogirou, O. Effect of low frequency magnetic fields on the growth of MNP-treated HT29 colon cancer cells. *Nanotechnology* **2018**, *29*, 175101. [CrossRef]
11. Goiriena-Goikoetxea, M.; Muñoz, D.; Orue, I.; Fernández-Gubieda, M.L.; Bokor, J.; Muela, A.; García-Arribas, A. Disk-shaped magnetic particles for cancer therapy. *Appl. Phys. Rev.* **2020**, *7*, 011306. [CrossRef]
12. Zhang, E.; Kircher, M.F.; Koch, M.; Eliasson, L.; Goldberg, S.N.; Renström, E. Dynamic magnetic fields remote-control apoptosis via nanoparticle rotation. *ACS Nano* **2014**, *8*, 3192–3201. [CrossRef] [PubMed]

13. Kim, D.H.; Rozhkova, E.A.; Ulasov, I.V.; Bader, S.D.; Rajh, T.; Lesniak, M.S.; Novosad, V. Biofunctionalized magnetic-vortex microdiscs for targeted cancer-cell destruction. *Nat. Mater.* **2010**, *9*, 165–171. [CrossRef] [PubMed]
14. Golovin, Y.I.; Golovin, D.Y.; Vlasova, K.Y.; Veselov, M.M.; Usvaliev, A.D.; Kabanov, A.V.; Klyachko, N.L. Non-Heating Alternating Magnetic Field Nanomechanical Stimulation of Biomolecule Structures via Magnetic Nanoparticles as the Basis for Future Low-Toxic Biomedical Applications. *Nanomaterials* **2021**, *11*, 2255. [CrossRef] [PubMed]
15. Golovin, Y.I.; Gribanovsky, S.L.; Golovin, D.Y.; Klyachko, N.L.; Majouga, A.G.; Master, A.M.; Sokolsky, M.; Kabanov, A.V. Towards nanomedicines of the future: Remote magneto-mechanical actuation of nanomedicines by alternating magnetic fields. *J. Control. Release* **2015**, *219*, 43–60. [CrossRef] [PubMed]
16. Available online: http://www.chemicell.com/products/protocols/fluidd/index.html (accessed on 28 December 2021).
17. Makridis, A.; Tziomaki, M.; Topouridou, K.; Yavropoulou, M.P.; Yovos, J.G.; Kalogirou, O.; Samaras, T. A novel strategy combining magnetic particle hyperthermia pulses with enhanced performance binary ferrite carriers for effective in vitro manipulation of primary human osteogenic sarcoma cells. *Int. J. Hyperthermia* **2016**, *32*, 778–785. [CrossRef]
18. Uzunova, V.; Tsiapla, A.R.; Stoyanova, T.; Myrovali, E.; Momchilova, A.; Kalogirou, O.; Tzoneva, R. Biocompatibility of iron oxide nanoparticles. *J. Chem. Technol. Metall.* **2021**, *56*, 1187–1191.
19. Creixell, M.; Bohorquez, A.C.; Torres-Lugo, M.; Rinaldi, C. EGFR-targeted magnetic nanoparticle heaters kill cancer cells without a perceptible temperature rise. *ACS Nano* **2011**, *5*, 7124–7129. [CrossRef]
20. Wang, M.H.; Chen, K.W.; Ni, D.X.; Fang, H.-J.; Jang, L.-S.; Chen, C.-H. Effect of extremely low frequency electromagnetic field parameters on the proliferation of human breast cancer. *Electromagn. Biol. Med.* **2021**, *40*, 384–392. [CrossRef]
21. Ispanixtlahuatl-Meráz, O.; Schins, R.P.F.; Chirino, Y.I. Cell type specific cytoskeleton disruption induced by engineered nanoparticles. *Environ. Sci. Nano* **2018**, *5*, 228–245. [CrossRef]
22. Tzoneva, R. Influence of electric field on cell behavior. Electrotreatment of cells for biomedical applications. *Asian J. Phys.* **2014**, *23*, 789–814.
23. Pehlivanova, V.; Tsoneva, I.; Tzoneva, R. Multiple effects of electroporation on the adhesive behavior of breast cancer cells and fibroblasts. *Cancer Cell Int.* **2012**, *9*, 9144.
24. Tzoneva, R.; Uzunova, V.; Apostolova, S.; Krüger-Genge, A.; Neffe, A.T.; Jung, F.; Lendlein, A. Angiogenic potential of endothelial and tumor cells seeded on gelatin–based hydrogels in response to electrical stimulations. *Clin. Hemorheol. Microcirc.* **2017**, *64*, 941–949. [CrossRef]
25. Master, A.; Williams, P.; Pothayee, N.; Zhang, R.; Vishwasrao, H.; Golovin, Y.I.; Riffle, J.S.; Sokolsky, M.; Kabanov, A.V. Remote Actuation of Magnetic Nanoparticles for Cancer Cell Selective Treatment through Cytoskeletal Disruption. *Sci. Rep.* **2016**, *6*, 33560. [CrossRef] [PubMed]
26. Zhang, L.; Ji, X.M.; Yang, X.X.; Zhang, X. Cell type- and density-dependent effect of 1 T static magnetic field on cell proliferation. *Oncotarget* **2017**, *8*, 13126–13141. [CrossRef]
27. Fan, Z.; Hu, P.; Xiang, L.; Liu, Y.; He, R.; Lu, T. A Static Magnetic Field Inhibits the Migration and Telomerase Function of Mouse Breast Cancer Cells. *Biomed Res. Int.* **2020**, *2020*, 7472618. [CrossRef]
28. Lin, T.; Wan, L.; Qi, X.; Shi, W.; Lin, J. A moderate static magnetic field enhances TRAIL-induced apoptosis by the inhibition of Cdc2 and subsequent downregulation of survivin in human breast carcinoma cells. *Bioelectromagnetics* **2014**, *35*, 337–346. [CrossRef] [PubMed]
29. Aljarrah, K.; Mhaidat, N.M.; Al-Akhras, M.A.H.; Aldaher, A.N.; Albiss, B.A.; Aledealat, K.; Alsheyab, F.M. Magnetic nanoparticles sensitize MCF-7 breast cancer cells to doxorubicin-induced apoptosis. *World J. Surg. Oncol.* **2012**, *10*, 62. [CrossRef]
30. Luo, Y.; Ji, X.; Liu, J.; Li, Z.; Wang, W.; Chen, W.; Wang, J.; Liu, Q.; Zhang, X. Moderate intensity static magnetic fields affect mitotic spindles and increase the antitumor efficacy of 5-FU and Taxol. *Bioelectrochemistry* **2016**, *109*, 31–40. [CrossRef]